

Spin-liquid behavior in $J_{\text{eff}} = \frac{1}{2}$ triangular lattice compound $\text{Ba}_3\text{IrTi}_2\text{O}_9$

Tusharkanti Dey,¹ A. V. Mahajan,^{1,*} P. Khuntia,² M. Baenitz,² B. Koteswararao,³ and F. C. Chou³

¹*Department of Physics, Indian Institute of Technology Bombay, Powai, Mumbai 400076, India*

²*Max Planck Institute for Chemical Physics of Solids, 01187 Dresden, Germany*

³*Center for Condensed Matter Sciences, National Taiwan University, Taipei 10617, Taiwan*

(Received 20 March 2012; revised manuscript received 24 August 2012; published 26 October 2012)

$\text{Ba}_3\text{IrTi}_2\text{O}_9$ crystallizes in a hexagonal structure consisting of a layered triangular arrangement of Ir^{4+} ($J_{\text{eff}} = \frac{1}{2}$). Magnetic susceptibility and heat capacity data show no magnetic ordering down to 0.35 K in spite of a strong magnetic coupling as evidenced by a large Curie-Weiss temperature $\theta_{\text{CW}} \sim -130$ K. The magnetic heat capacity follows a power law at low temperature. Our measurements suggest that $\text{Ba}_3\text{IrTi}_2\text{O}_9$ is a $5d$, Ir-based ($J_{\text{eff}} = \frac{1}{2}$), quantum spin liquid on a two-dimensional (2D) triangular lattice.

DOI: [10.1103/PhysRevB.86.140405](https://doi.org/10.1103/PhysRevB.86.140405)

PACS number(s): 75.40.Cx, 75.45.+j, 75.47.Lx

Introduction. Since Anderson proposed the resonating valence bond model,¹ researchers have been searching for experimental realizations of quantum spin liquids (QSL)² in geometrically frustrated magnets. In such materials, incompatibility of local interactions, called frustration, leads to a strong enhancement of quantum spin fluctuations and effectively suppresses the long-range magnetic ordering. As a result, the material remains paramagnetic down to very low temperatures compared to the Curie-Weiss (CW) temperature θ_{CW} . The frustration in these materials often arises from some special geometries like triangular, kagome, pyrochlore, garnet, etc.³

The spin liquid candidates found so far have been mostly $3d$ transition-metal-based materials. A few examples are two-dimensional (2D) kagome systems $\text{SrCr}_9\text{P}_4\text{Ga}_{12-9p}\text{O}_{19}$ ($S = \frac{3}{2}$),⁴ and $\text{ZnCu}_3(\text{OH})_6\text{Cl}_2$ ($S = \frac{1}{2}$),⁵ $S = 1$ 2D triangular lattice antiferromagnet NiGa_2S_4 ,⁶ and organic materials like $S = \frac{1}{2}$ triangular lattice κ -(ET)₂ $\text{Cu}_2(\text{CN})_3$.⁷ There are very few examples of spin liquid systems with $4d$ or $5d$ spins. $\text{Na}_4\text{Ir}_3\text{O}_8$,⁸ a $S = \frac{1}{2}$ spin liquid in a three-dimensional (3D) hyperkagome network, is probably the most notable member of the $5d$ spin liquid family.

Recently, $\text{Ba}_3\text{CuSb}_2\text{O}_9$ ($S = \frac{1}{2}$) with hexagonal space group $P6_3mc$ was suggested to be in the QSL ground state.⁹ High-pressure hexagonal ($P6_3mc$, 6H-B) and cubic ($Fm-3m$, 3C) phases of $\text{Ba}_3\text{NiSb}_2\text{O}_9$ have also been suggested to be in the 2D and 3D QSL ground states, respectively.¹⁰

We have been searching for QSL candidates among hexagonal oxides with $4d/5d$ elements instead of $3d$ elements. The $5d$ materials are very different from $3d$ materials and thus interesting because of a weak onsite Coulomb energy but a strong spin-orbit coupling. For example, Sr_2IrO_4 ¹¹ and Ba_2IrO_4 ¹² are reported to be spin-orbit-driven Mott insulators. The magnetic properties of these systems have been described based on a $J_{\text{eff}} = \frac{1}{2}$ state for the Ir^{4+} ion. Among the various Ir-based compounds, $\text{Ba}_3\text{IrTi}_2\text{O}_9$ is rather interesting since it has a chemical formula similar to the Cu- and Ni-based compounds (discussed in the previous paragraph) and it crystallizes in a hexagonal structure.¹³ However, detailed structural parameters have not been reported. Bryne *et al.*¹³ reported magnetic susceptibility of $\text{Ba}_3\text{IrTi}_2\text{O}_9$ in the temperature range 77–600 K. High antiferromagnetic Weiss temperature ($|\theta_{\text{CW}}| > 400$ K) was obtained by them, suggesting that the magnetic Ir^{4+} ions are strongly coupled with each other. An obvious

question arises: Do they order at lower temperatures? If not, then is it a spin liquid system and a $5d$ analog of $\text{Ba}_3\text{CuSb}_2\text{O}_9$?

Here we report preparation, structural analysis, magnetic susceptibility, and specific heat measurements on $\text{Ba}_3\text{IrTi}_2\text{O}_9$. It crystallizes in space group $P6_3mc$ like $\text{Ba}_3\text{CuSb}_2\text{O}_9$ and the 6H-B phase of $\text{Ba}_3\text{NiSb}_2\text{O}_9$. A large negative θ_{CW} is obtained from CW fitting of susceptibility data, but no magnetic ordering is found from susceptibility and heat capacity measurements down to 0.35 K. Magnetic heat capacity follows a power law at low temperatures. This indicates that the system is highly frustrated and an example of a $5d$ QSL. We suggest that this is the first candidate of a $5d$ -based quantum spin liquid on a 2D triangular lattice with $J_{\text{eff}} = \frac{1}{2}$.

Experimental details. Polycrystalline sample of $\text{Ba}_3\text{IrTi}_2\text{O}_9$ was prepared by conventional solid-state reaction method using high purity (99.9%) starting materials.

Powder x-ray diffraction (XRD) measurements were performed at room temperature with $\text{Cu } K_\alpha$ radiation ($\lambda = 1.54182$ Å) in a PANalytical X'Pert PRO diffractometer. Magnetization measurements were performed in a Quantum Design SQUID vibrating sample magnetometer (SVSM). Heat capacity measurements were carried out in the temperature range 0.35–295 K and field range 0–9 T in a Quantum Design physical properties measurement system (PPMS). High temperature (up to 800 K) susceptibility was measured using a PPMS VSM.

Results and discussion. XRD measurement was done to check the phase purity of the sample and to determine crystal parameters, as the parameters were not mentioned in the earlier report.¹³ The Ru analog of $\text{Ba}_3\text{IrTi}_2\text{O}_9$, $\text{Ba}_3\text{RuTi}_2\text{O}_9$, has been mentioned in literature and it crystallizes in the hexagonal $P6_3mc$ space group.¹⁴ On the other hand, with a different Ir and Ti ratio, $\text{Ba}_3\text{TiIr}_2\text{O}_9$ has been suggested to crystallize in the space group $P6_3/mmc$.¹⁵ In both these space groups metal-metal structural dimers ($2b$ sites or $4f$ site) are separated by the $2a$ site metal plane. In $P6_3mc$, the metal ions within the dimer are ordered while in the $P6_3/mmc$ space group the metal ions within the dimers are not ordered. We tried to refine our XRD data using these space groups and found $P6_3mc$ gives better refinement with a large site sharing by the Ti^{4+} and Ir^{4+} ions (see the Supplemental Material).¹⁶ The lattice constants obtained from refinement are $a = b = 5.7214$ Å and $c = 14.0721$ Å.

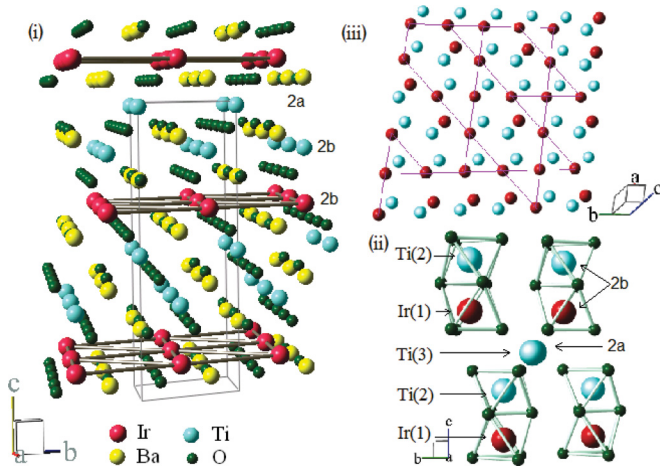


FIG. 1. (Color online) (i) Structure of $\text{Ba}_3\text{IrTi}_2\text{O}_9$ without any site disorder between Ti^{4+} and Ir^{4+} . The triangular arrangement of Ir^{4+} spins in the ab plane is shown. (ii) IrTiO_9 dimers are shown. (iii) One possible arrangement of Ti^{4+} and Ir^{4+} ions in the ab plane is shown when about $\frac{1}{3}$ of Ir^{4+} ions from $\text{Ir}(1)$ site are exchanged with Ti^{4+} ions of the $\text{Ti}(2)$ site.

In the ideal case (i.e., without any site disorder), the $\text{Ti}(3)$ site is occupied by Ti^{4+} ions and the $\text{Ti}(2)$ and $\text{Ir}(1)$ sites are occupied by distinct metal ions Ti^{4+} and Ir^{4+} ions, respectively. This is indeed (nearly) the situation in $\text{Ba}_3\text{CuSb}_2\text{O}_9$, where the Cu site is occupied only by Cu^{2+} (leaving aside a 5% site disorder), and Sb^{5+} ions are located at $\text{Sb}(1)$ and $\text{Sb}(2)$ sites. However in our case, we found a $(37 \pm 10)\%$ site sharing of Ir^{4+} ions with Ti^{4+} ions between $\text{Ir}(1)$ and $\text{Ti}(2)$ sites and $(7 \pm 4)\%$ site sharing with Ti^{4+} ions in the $\text{Ti}(3)$ site. This is in fact not unexpected, as their ionic radii are very similar. Sakamoto *et al.* also found 21% site sharing between Ti^{4+} and Ir^{4+} in $\text{Ba}_3\text{TiIr}_2\text{O}_9$ ¹⁵ and a similar site-disordered situation was reported in the case of $\text{Ba}_3\text{RuTi}_2\text{O}_9$ by Radtke *et al.*¹⁷ They studied probability of different Ru^{4+} and Ti^{4+} combinations based on high-resolution electron energy loss spectroscopy and first-principles band structure calculations and concluded that site sharing of ions in $2b$ sites [i.e., $\text{Ir}(1)$ and $\text{Ti}(2)$ sites in our case] is more probable while site sharing with $2a$ sites [i.e., $\text{Ir}(1)$ and $\text{Ti}(3)$ sites in our case] is less probable. This was suggested because structural dimers of like ions (Ti-Ti) are energetically unfavorable because of a strong Ti-Ti repulsion. The same reason is probably valid in our case and results in a small 7% site sharing between Ir^{4+} ions at the $\text{Ir}(1)$ site and Ti^{4+} ions at the $\text{Ti}(3)$ site.

In the case of perfect ordering among Ti^{4+} and Ir^{4+} , these two ions form face-sharing IrTiO_9 bioctahedra [shown in Fig. 1(ii)] and Ir^{4+} spins form an edge-shared triangular lattice in the ab plane, as shown in Fig. 1. As a consequence of site disorder, the edge-shared triangular planes will be depleted. Further, Ir occupying the $\text{Ti}(2)$ sites might also form a depleted triangular plane. A possible arrangement is shown in Fig. 1(iii). The blue (light gray) atoms represent Ti and the red (dark gray) atoms are Ir .

Zero-field-cooled (ZFC) and field-cooled (FC) magnetic susceptibility was measured with different fields in the temperature range 2–400 K. No magnetic ordering is found down to 2 K but with 100 Oe field ZFC-FC splitting is

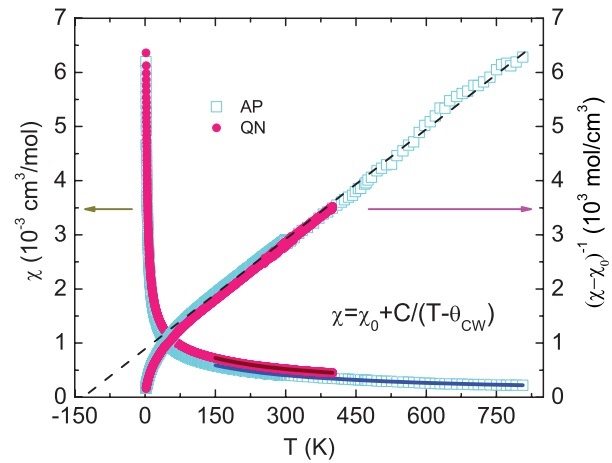


FIG. 2. (Color online) Left axis: Magnetic susceptibilities of as-prepared (AP) and quenched (QN) $\text{Ba}_3\text{IrTi}_2\text{O}_9$ samples are shown. Solid lines denote fitting with CW law in high-temperature range >150 K. Right axis: Inverse susceptibilities (after subtracting χ_0) as function of temperature for both AP and QN. The dashed line is a linear extrapolation of the high-temperature data of the AP sample.

seen below 80 K (shown in Fig. 4 of the Supplemental Material).¹⁶ However, the splitting is very small (only 11% of total magnetization at 2 K) and suppressed when measured even with 500 Oe. This suggests that a small fraction of the spins take part in a glassy state while the majority of the spins do not. In $\text{Na}_4\text{Ir}_3\text{O}_8$ also a small ZFC-FC ($<10\%$ of total magnetization) splitting was observed below 6 K, which the authors concluded came from a small fraction of the spins.⁸ Figure 2 shows the temperature (T) dependence of dc magnetic susceptibility of the as-prepared sample (light blue [light gray] open squares). Data obtained with field 5 kOe using a SVSM (2–300 K) and using a VSM with a high-temperature attachment with field 50 kOe (300–800 K) have been shown together. Susceptibility data can be fitted well with the CW formula in the high temperature (150–800 K) region (shown in Fig. 2), which yields temperature-independent susceptibility $\chi_0 = 0.61 \times 10^{-4} \text{ cm}^3/\text{mol}$, Curie constant $C = 0.149 \text{ cm}^3 \text{ K}/\text{mol}$ and $\theta_{\text{CW}} = -133 \text{ K}$. In many Ir -based oxides χ_0 is found to be large and varies within a wide range.^{15,18} The C value obtained from fitting is much less than that expected for $S = \frac{1}{2}$ magnetic moments ($0.375 \text{ cm}^3 \text{ K}/\text{mol}$) value. The large θ_{CW} value suggests that there still are significant correlations in the triangular planes despite the depletion. The suppression of magnetic moments could be an effect of the extended nature of the $5d$ orbitals and the strong spin-orbit coupling expected for $5d$ transition-metal oxides. Indeed, in the magnetically ordered iridates such as Sr_2IrO_4 , the low-temperature saturation moments have been found to be less than one tenth of a μ_B and effective moment in the paramagnetic region is found to be $\sim 0.4 \mu_B$.¹⁹

With the aim of investigating how the preparation procedure might affect the site ordering and hence the magnetic properties, we quenched the as-prepared (AP) sample in liquid nitrogen from 1000°C . Comparing the normalized x-ray diffraction pattern of both AP and quenched (QN) samples, we found that width of all the peaks and peak height of many

peaks are decreased in the QN sample. This indicates that the crystal symmetry is unchanged but ionic disorder (and possibly distortions) are less in the QN sample compared to the AP sample. Refinement of XRD pattern is consistent with a $\sim 35\%$ site disorder between Ir^{4+} and Ti^{4+} cations at the $2b$ site but without any site sharing with the $2a$ site Ti^{4+} cations. We also found a marginal increase in the lattice constants with $a = b = 5.7216 \text{ \AA}$ and $c = 14.0768 \text{ \AA}$. Susceptibility for the QN sample measured with field 5 kOe in the temperature range 2–400 K (Fig. 2) shows no sign of magnetic ordering. Data fitted to CW law in the temperature range 150–400 K yields $\chi_0 = 1.68 \times 10^{-4} \text{ cm}^3/\text{mol}$, $C = 0.145 \text{ cm}^3 \text{ K}/\text{mol}$, and $\theta_{\text{CW}} = -111 \text{ K}$. The θ_{CW} is somewhat smaller than in the AP sample, while C is nearly unchanged. Inverse susceptibilities (after subtracting the temperature-independent part χ_0) of AP and QN samples are linear in temperature and deviate from linearity below $\sim 80 \text{ K}$, as shown on the right axis of Fig. 2.

The large, negative θ_{CW} indicates that Ir^{4+} magnetic moments are strongly antiferromagnetically coupled with each other. Apparently something prevents long-range magnetic ordering to set in even at 0.35 K (evident from heat capacity measurement), which is nearly four hundred times lower than θ_{CW} . This suggests that in spite of the depletion of magnetic ions from the triangular planes, geometrical frustration continues to exist in the depleted triangular lattice and plays a dominant role in determining the magnetic properties of this system. Note that a part of the Curie term could be arising from a few percent of uncorrelated Ir^{4+} spins (and possibly some Ti^{3+} as well) present in the system, which we call orphan spins (discussed later).

One should note that in literature that $|\theta_{\text{CW}}|$ and μ_{eff} reported for $\text{Ba}_3\text{IrTi}_2\text{O}_9$ are greater than 400 K and $1.73 \mu_B$, respectively,¹³ which is at variance from our data. To clarify this discrepancy, we have fitted the published data (Fig. 5 of Ref. 16) with CW law and found $\chi_{0B} = 3.42 \times 10^{-4} \text{ cm}^3/\text{mol}$, $C = 0.10 \text{ cm}^3\text{K}/\text{mol}$ ($\mu_{\text{eff}} = 0.89\mu_B$) and $\theta_{\text{CW}} = -104 \text{ K}$. Apparently, Bryne *et al.* used $\chi_{0A} = 0.5 \times 10^{-4} \text{ cm}^3/\text{mol}$ leading them to infer a different θ_{CW} and μ_{eff} (see Ref. 16 for details).

Next, in Fig. 3 we present the heat capacity (C_P) in various fields for the AP and QN samples (data for all fields are shown in the Supplemental Material).¹⁶ No anomaly indicative of long-range ordering is found in the measurement range (0.35–295 K). For both the samples, C_P depends on the applied field below $\sim 20 \text{ K}$. This field dependence could arise from a Schottky anomaly of orphan spins. We model the heat capacity of $\text{Ba}_3\text{IrTi}_2\text{O}_9$ as arising out of four contributions. These are namely the magnetic contribution of the correlated spins (C_M), the lattice contribution (C_{lat}), the Schottky anomaly of the orphan spins ($C_{\text{Sch-orp}}$), and the nuclear Schottky anomaly ($C_{\text{Sch-nuc}}$). To extract the magnetic part of the heat capacity arising from correlated magnetic moments, we proceed as follows. The C_P has contributions from C_M , C_{lat} , the Schottky anomaly ($C_{\text{Sch-orp}}$) from Ir orphan spins, and nuclear Schottky anomaly ($C_{\text{Sch-nuc}}$). C_{lat} is field independent while the others might be field dependent. Using the zero-field heat capacity [$C_P(0 \text{ T})$] and that measured with the nT field [$C_P(n\text{T})$], we obtain $\Delta C_{P-\text{Ir}}/T = [C_P(n\text{T}) - C_P(0\text{T})]/T$. This is then fitted with $f[C_{\text{Sch}}(\Delta_1) - C_{\text{Sch}}(\Delta_2)]/T$, where f is

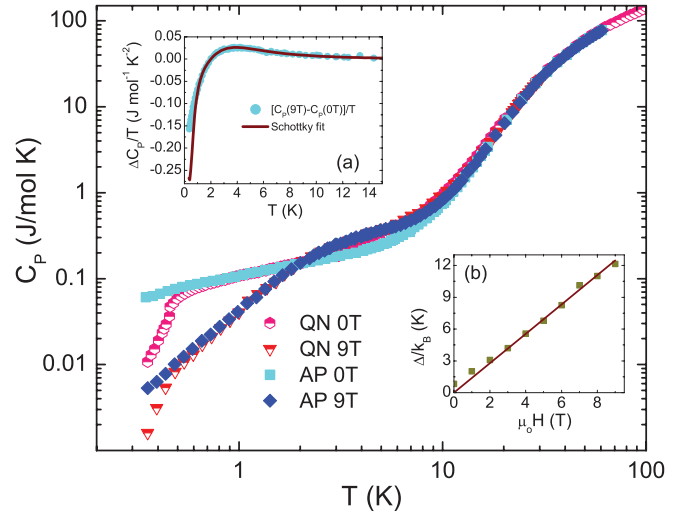


FIG. 3. (Color online) Heat capacity of AP and QN $\text{Ba}_3\text{IrTi}_2\text{O}_9$ sample measured in various applied magnetic fields are shown in a log-log scale. Inset: (a) Solid circles represent $[C_P(9 \text{ T}) - C_P(0 \text{ T})]/T$ of the AP sample and the solid line is the fit (see the text). (b) Δ/k_B as a function of $\mu_0 H$ from 0T to 9T is shown and the solid line is a fit to Zeeman splitting.

the percentage of orphan spins present in the sample. $C_{\text{Sch}}(\Delta_1)$ and $C_{\text{Sch}}(\Delta_2)$ are the Schottky anomalies from $S = \frac{1}{2}$ spins and Δ_1 and Δ_2 are the level splittings with applied magnetic fields H_1 and H_2 , respectively. Here,

$$C_{\text{Sch}}(\Delta) = R \left(\frac{\Delta}{k_B T} \right)^2 \frac{\exp\left(\frac{\Delta}{k_B T}\right)}{\left[1 + \exp\left(\frac{\Delta}{k_B T}\right)\right]^2}, \quad (1)$$

where R is the universal gas constant and k_B is the Boltzman constant. Inset (a) of Fig. 3 shows $\Delta C_{P-\text{Ir}}/T$ obtained for 0T and 9T along with the fit described above. The good fit above $\sim 2 \text{ K}$ suggests that C_M is not field dependent at least above $\sim 2 \text{ K}$ and all the field dependence is in $C_{\text{Sch-orp}}$. However, below $\sim 2 \text{ K}$, there is deviation of the fit from the data (this is much larger than the expected nuclear Schottky anomaly), which suggests the C_M might be field dependent there. The fraction of orphan spins f is found to be $\sim 3\%$. The Schottky splitting (Δ/k_B) obtained from fitting for different fields is plotted as a function of field in inset (b) of Fig. 3. Similar analysis has been reported for $\text{Ba}_3\text{CuSb}_2\text{O}_9$,⁹ $\text{ZnCu}_3(\text{OH})_6\text{Cl}_2$,²⁰ and Y_2BaNiO_5 .²¹ At zero field also we found a level splitting of 1.8 K which is unexpected but found in $\text{Ba}_3\text{CuSb}_2\text{O}_9$ ⁹ as well. For $\mu_0 H \geq 2\text{T}$, the Schottky splitting gap follows $\Delta = g\mu_B H$, as expected for free spin Schottky anomalies. The g value for orphan spins obtained from the linear fit is 2.06.

Using Eq. (1), the Schottky heat capacity can now be subtracted from the measured heat capacity of $\text{Ba}_3\text{IrTi}_2\text{O}_9$. Next, we extract the lattice heat capacity and for that we have used $\text{Ba}_3\text{ZnSb}_2\text{O}_9$ as a nonmagnetic analog. Since the Debye frequency is primarily determined by the lighter atoms (in these cases oxygen), it will not vary much between these two. The high-temperature heat capacities of $\text{Ba}_3\text{IrTi}_2\text{O}_9$ and $\text{Ba}_3\text{ZnSb}_2\text{O}_9$ differ because of the difference in their molecular weights and lattice volumes. By scaling the heat capacity of $\text{Ba}_3\text{ZnSb}_2\text{O}_9$ (obtained from Ref. 9) by a factor of ~ 0.75 we

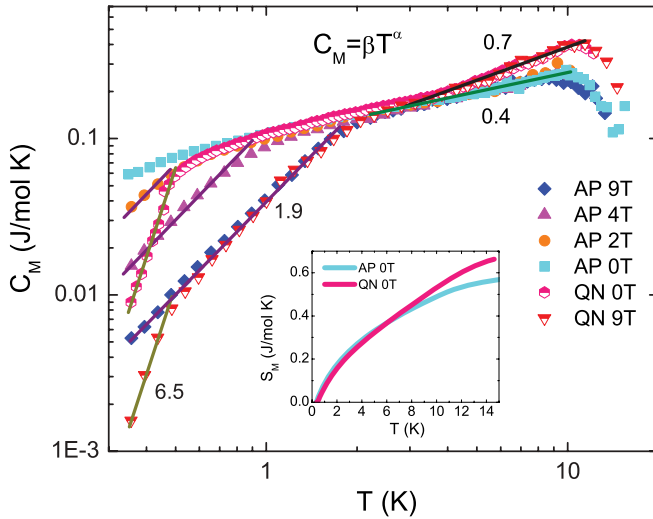


FIG. 4. (Color online) Magnetic heat capacity for the AP and the QN samples are shown. The solid lines are fit to power law with power indicated in the figure. In the low-temperature region, solid lines with similar colors have the same power. Inset: Magnetic entropy change ΔS_M is shown as a function of temperature for 0T.

find that the heat capacities of $\text{Ba}_3\text{ZnSb}_2\text{O}_9$ and $\text{Ba}_3\text{IrTi}_2\text{O}_9$ match in the temperature region ~ 20 – 30 K. The scaled heat capacity of $\text{Ba}_3\text{ZnSb}_2\text{O}_9$ is then subtracted from that of $\text{Ba}_3\text{IrTi}_2\text{O}_9$ in order to obtain the magnetic heat capacity as shown in Fig. 4.

The C_M for both AP and QN samples is independent of field from ~ 2.5 – 10 K, and in this range they follow a power law in temperature with power ~ 0.4 for the AP sample and ~ 0.7 for the QN sample. Above ~ 10 K the results can be largely affected by uncertainties associated with the subtraction process. Notably, C_M for the QN sample is larger than that for the AP sample. Below ~ 2 K, C_M becomes field dependent (for both samples) but follows power law with temperature with the same power for different fields. This power is 1.9 for the AP sample and 6.5 for the QN sample at very low temperature (shown in Fig. 4). From the heat capacity data of $\text{Ba}_3\text{CuSb}_2\text{O}_9$ (with space group $P6_3/mmc$) published in Ref. 22, we have extracted C_M by subtracting a Schottky contribution. Here also we found C_M to be field dependent below ~ 2 K but following a power law with power 2.1 for different fields, and field independent in the range 5–15 K (see the Supplemental Material).¹⁶ In many other frustrated systems C_M follows power law with temperature. The power is 2 for 2D $S = 1$ system NiGa_2S_4 ,⁶ 1 and 2 for $\text{Ba}_3\text{NiSb}_2\text{O}_9$ 6H-B and 3C phases respectively,¹⁰ between 2 and 3 for $\text{Na}_4\text{Ir}_3\text{O}_8$,⁸ and 1 at low temperature but 2 at higher temperature in the $S = \frac{1}{2}$ system $\text{Ba}_3\text{CuSb}_2\text{O}_9$ (with space group $P6_3/mc$).⁹ A power of $\frac{2}{3}$ was predicted by Motrunich²³ for $S = \frac{1}{2}$ triangular lattice

organic spin liquid system κ -(ET)₂ $\text{Cu}_2(\text{CN})_3$. In view of the fact that our Ir-based system is expected to have a significant spin-orbit coupling, fresh theoretical effort in this direction is warranted.

Magnetic entropy change (ΔS_M) is obtained by integration of C_M/T with T and is shown as a function of temperature in the inset of Fig. 4. The ΔS_M is an order of magnitude lower than $R\ln 2$ expected for ordered $S = \frac{1}{2}$ systems. In many geometrically frustrated systems it is observed that the entropy change is lower than the expected value. For example, the entropy change is 30% and 41% of $R\ln(2S + 1)$ for $\text{Ba}_3\text{CuSb}_2\text{O}_9$ and $\text{Ba}_3\text{NiSb}_2\text{O}_9$ (6H-B phase) respectively, which are similar in structure to $\text{Ba}_3\text{IrTi}_2\text{O}_9$. However, in $\text{Ba}_3\text{IrTi}_2\text{O}_9$ the magnetic moments are strongly reduced, probably due to a strong spin-orbit coupling. Here S is not a good quantum number and probably J_{eff} is, so the expected entropy change may not be $R\ln(2S + 1)$ (i.e., $R\ln 2$) but rather a much smaller quantity. Interestingly, the heat capacity is different for the QN sample than for the AP sample, implying the influence of atomic site disorder on the details of the triangular lattice and hence the ground state.

Conclusions. We have presented a potentially new spin liquid system $\text{Ba}_3\text{IrTi}_2\text{O}_9$, which is based on a triangular lattice of Ir^{4+} ions with electrons responsible for the magnetic properties coming from the $5d$ electronic orbital. The sample crystallizes in $P6_3mc$ space group with a large disorder between Ti^{4+} and Ir^{4+} cations, resulting in a site dilution of nearly $\frac{1}{3}$ of the Ir^{4+} sites of the edge-shared triangular plane by nonmagnetic Ti^{4+} . Apparently, magnetic correlations and frustrations are still maintained with the absence of magnetic ordering down to 0.35 K in spite of a high θ_{CW} value (approx. -130 K). Associated with this is a magnetic heat capacity, which, although field dependent, follows a power law with power 1.9 in the low-temperature range. The QN sample has a different behavior. This is somewhat like in $\text{Ba}_3\text{CuSb}_2\text{O}_9$, where different atomic arrangements (Refs. 9 and 22) give rise to different magnetic heat capacities. As Nakatsuji *et al.*²² has reported that due to site sharing between Cu^{2+} and Sb^{5+} ions, a distorted honeycomb lattice is formed in $\text{Ba}_3\text{CuSb}_2\text{O}_9$, we speculate that a similar situation may occur in $\text{Ba}_3\text{IrTi}_2\text{O}_9$ yet maintaining a spin liquid ground state. With the demonstration of the existence of a $J_{\text{eff}} = \frac{1}{2}$ state (having a large spin-orbit coupling) in Sr_2IrO_4 ,²⁴ $\text{Ba}_3\text{IrTi}_2\text{O}_9$ is possibly an example of a $J_{\text{eff}} = \frac{1}{2}$ quantum spin liquid system and a $5d$ analog of $\text{Ba}_3\text{CuSb}_2\text{O}_9$. This should open up a new area pertinent to the search for exotic magnetic behavior in $5d$ transition-metal-based compounds.

Acknowledgement. We thank the Department of Science and Technology, government of India, for financial support. F.C.C. acknowledges the support from the National Science Council of Taiwan under Project No. NSC-100-2119-M-002-021.

*mahajan@phy.iitb.ac.in

¹P. W. Anderson, *Mater. Res. Bull.* **8**, 153 (1973).

²L. Balents, *Nature (London)* **464**, 199 (2010).

³For a review, see *Introduction to Frustrated Magnetism*, edited by C. Lacroix, P. Mendels, and F. Mila (Springer, Heidelberg, 2010).

- ⁴A. P. Ramirez, B. Hesse, and M. Winklemann, *Phys. Rev. Lett.* **84**, 2957 (2000).
- ⁵J. S. Helton, K. Matan, M. P. Shores, E. A. Nytko, B. M. Bartlett, Y. Yoshida, Y. Takano, A. Suslov, Y. Qiu, J.-H. Chung, D. G. Nocera, and Y. S. Lee, *Phys. Rev. Lett.* **98**, 107204 (2007); P. Mendels, F. Bert, M. A. de Vries, A. Olariu, A. Harrison, F. Duc, J. C. Trombe, J. S. Lord, A. Amato, and C. Baines, *ibid.* **98**, 077204 (2007).
- ⁶S. Nakatsuji, Y. Nambu, H. Tonomura, O. Sakai, S. Jonas, C. Broholm, H. Tsunetsugu, Y. Qiu, and Y. Maeno, *Science* **309**, 1697 (2005).
- ⁷Y. Shimizu, K. Miyagawa, K. Kanoda, M. Maesato, and G. Saito, *Phys. Rev. Lett.* **91**, 107001 (2003).
- ⁸Y. Okamoto, M. Nohara, H. Aruga-Katori, and H. Takagi, *Phys. Rev. Lett.* **99**, 137207 (2007).
- ⁹H. D. Zhou, E. S. Choi, G. Li, L. Balicas, C. R. Wiebe, Y. Qiu, J. R. D. Copley, and J. S. Gardner, *Phys. Rev. Lett.* **106**, 147204 (2011).
- ¹⁰J. G. Cheng, G. Li, L. Balicas, J. S. Zhou, J. B. Goodenough, C. Xu, and H. D. Zhou, *Phys. Rev. Lett.* **107**, 197204 (2011).
- ¹¹B. J. Kim, H. Jin, S. J. Moon, J.-Y. Kim, B.-G. Park, C. S. Leem, J. Yu, T. W. Noh, C. Kim, S.-J. Oh, J.-H. Park, V. Durairaj, G. Cao, and E. Rotenberg, *Phys. Rev. Lett.* **101**, 076402 (2008).
- ¹²H. Okabe, M. Isobe, E. Takayama-Muromachi, A. Koda, S. Takeshita, M. Hiraishi, M. Miyazaki, R. Kadono, Y. Miyake, and J. Akimitsu, *Phys. Rev. B* **83**, 155118 (2011).
- ¹³R. C. Byrne and C. W. Moeller, *J. Solid State Chem.* **2**, 228 (1970).
- ¹⁴C. Maunders, J. Etheridge, N. Wright, and H. J. Whitfield, *Acta Crystallogr. Sect. B* **61**, 154 (2005).
- ¹⁵T. Sakamoto, Y. Doi, and Y. Hinatsu, *J. Solid State Chem.* **179**, 2595 (2006).
- ¹⁶See Supplemental Material at <http://link.aps.org/supplemental/10.1103/PhysRevB.86.140405> for details of structural, heat capacity and magnetization data and analysis.
- ¹⁷G. Radtke, C. Maunders, A. Saul, S. Lazar, H. J. Whitfield, J. Etheridge, and G. A. Botton, *Phys. Rev. B* **81**, 085112 (2010).
- ¹⁸Y. Singh and P. Gegenwart, *Phys. Rev. B* **82**, 064412 (2010).
- ¹⁹S. Chikara, O. Korneta, W. P. Crummett, L. E. DeLong, P. Schlottmann, and G. Cao, *Phys. Rev. B* **80**, 140407(R) (2009).
- ²⁰M. A. de Vries, K. V. Kamenev, W. A. Kockelmann, J. Sanchez-Benitez, and A. Harrison, *Phys. Rev. Lett.* **100**, 157205 (2008).
- ²¹A. P. Ramirez, S. W. Cheong, and M. L. Kaplan, *Phys. Rev. Lett.* **72**, 3108 (1994).
- ²²S. Nakatsuji, K. Kuga, K. Kimura, R. Satake, N. Katayama, E. Nishibori, H. Sawa, R. Ishii, M. Hagiwara, F. Bridges, T. U. Ito, W. Higemoto, Y. Karakai, M. Halim, A. A. Nugroho, J. A. Rodriguez-Rivera, M. A. Green, and C. Broholm, *Science* **336**, 559 (2012).
- ²³O. I. Motrunich, *Phys. Rev. B* **72**, 045105 (2005).
- ²⁴B. J. Kim, H. Ohsumi, T. Komesu, S. Sakai, T. Morita, H. Takagi, and T. Arima, *Science* **323**, 1329 (2009).